Biochemical Journal Immediate Publication. Published on 6 Mar 2007 as manuscript BJ20061681

The mechanism of addition of pyridoxal 5'-phosphate to *Escherichia coli* apo-serine hydroxymethyltransferase

Francesca Malerba, Andrea Bellelli, Alessandra Giorgi, Francesco Bossa and Roberto Contestabile[§]

Dipartimento di Scienze Biochimiche "A. Rossi Fanelli", Università degli Studi di Roma "La Sapienza", Piazzale Aldo Moro 5, 00185 Roma, Italy

Running Title: Addition of PLP to apo-serine hydroxymethyltransferase

Key Words: Pyridoxal phosphate, serine hydroxymethyltransferase, cofactor addition, folding pathway, fold-type I enzymes

[§]To whom correspondence should be addressed: Roberto Contestabile, Dipartimento di Scienze Biochimiche, Università degli Studi di Roma "La Sapienza", Piazzale Aldo Moro 5, 00185 Roma, Italy, Tel. +39 0649917569; Fax +39 0649917566; E-Mail: roberto.contestabile@uniroma1.it

Abbreviations: PLP, pyridoxal 5'-phosphate; PNP, pyridoxine 5'-phosphate; *e*SHMT, *Escherichia coli* serine hydroxymethyltransferase; H_4PteGlu, tetrahydropteroylglutamate.

SUMMARY

Previous studies suggest that the addition of pyridoxal 5'-phosphate to apo-serine hydroxymethyltransferase from *Escherichia coli* is the last event in the enzyme's folding process. We propose a mechanism for this reaction based on quenched-flow, stopped-flow and rapid scanning stopped-flow experiments. All experiments were performed with an excess of apo-enzyme over cofactor, since excess pyridoxal phosphate results in a second molecule of cofactor binding to Lys346, which is part of the tetrahydropteroylglutamate binding site. The equilibrium between the aldehyde and hydrate forms of the cofactor affects the kinetics of addition to the active site. Direct evidence of the formation of an intermediate aldimine between the cofactor and the active site lysine was obtained. The results have been interpreted according to a three-step mechanism in which: 1) both aldehyde and hydrate forms of the cofactor bind rapidly and non-covalently to the apo-enzyme; 2) only the aldehyde form reacts with the active site lysine to give an intermediate internal aldimine with unusual spectral properties; 3) a final conformational change gives the native holo-enzyme.

Biochemical Journal Immediate Publication. Published on 6 Mar 2007 as manuscript BJ20061681

INTRODUCTION

The encounter between cofactors and apo-proteins in the cell is a crucial event that can occur at different stages of polypeptide folding and affect it to a variable extent [1, 2]. The form in which the cofactor is available in the intracellular medium may also differ according to its reactivity or toxicity [3]. The role of pyridoxal 5'-phosphate (PLP) in folding and structural stabilisation apparently varies among the enzymes which use it as cofactor [4-8]. This is not surprising, considering that there are at least five evolutionary unrelated families of such enzymes, corresponding to completely different protein folds (fold-types I-V) [9].

The mechanism of PLP homeostasis and targeting to the newly synthesised apo-enzymes is largely unknown. A first step in elucidating this process is to understand how PLP reacts *in vitro* with a purified PLP-dependent apo-enzyme, to form the active holo-enzyme. We have chosen *Escherichia coli* and its serine hydroxymethyltransferase (*e*SHMT) (fold-type I) as our model system because of: i) the known intracellular distribution and concentration of the B_6 vitamers in *E. coli* [10]; ii) the knowledge of the folding mechanism of *e*SHMT and its relationship to the addition of PLP [8, 11-13]; iii) the availability of a number of important site-specific mutants of *e*SHMT; iv) the published high resolution structure of the holo-enzyme [14].

The mechanism of addition of PLP to several different fold-type I apo-enzymes has been previously investigated for aspartate aminotransferase, glutamate decarboxylase and tryptophanase [15-19]. These studies suggested a three-step mechanism, but were unable to identify unambiguously the structure of the intermediates. Since these studies were performed, advances in rapid scanning spectrophotometry and in the knowledge of folding mechanisms have provided a new impetus to further research efforts.

The folding mechanism of *e*SHMT has been investigated in detail and is understood better than that of any other fold-type I PLP-dependent enzyme. It may be divided into two phases. In the first, relatively rapid phase, two domains fold into their native state, forming an intermediate that has virtually all of the native secondary structure, exhibits most of the native tertiary structure, is a dimer, but is not able to bind PLP. In this intermediate, the N-terminus and an inter-domain segment remain exposed to solvent. In the slow phase, the intermediate is converted into the apo-enzyme, which is able to bind PLP. Inspection of the crystal structure of the holo-enzyme shows that PLP is buried in a deep cavity with no obvious route of entrance or escape to the solvent [14]. Thus, in the apo-enzyme the active site entrance must be more accessible than in the holo-enzyme.

The present work determines the mechanism of addition of PLP to apo-*e*SHMT and the absorption spectra of all kinetic species involved. The effect of the equilibrium between hydrate and aldehyde cofactor on the kinetics of holo-enzyme formation is also determined. Future studies will focus on cofactor specificity and the structure of the protein in all steps of the proposed mechanism. These will use *e*SHMT site-specific mutants and aldimine complexes of PLP with substrate and non-substrate amino acids.

Biochemical Journal Immediate Publication. Published on 6 Mar 2007 as manuscript BJ20061681

EXPERIMENTAL PROCEDURES

Materials - Ingredients for bacterial growth were from Sigma-Aldrich. Chemicals for the purification of the enzymes were from BDH; DEAE-Sepharose and Phenyl-Sepharose from GE Healthcare. Alcohol dehydrogenase was from Sigma-Aldrich. *e*SHMT and methylenetetrahydrofolate dehydrogenase were purified as previously described [20, 21]. (6*S*) H_4PteGlu, was a gift from Eprova AG, Schaffhausen, Switzerland. PLP was from Sigma-Aldrich (98% pure). All other reagents were from Sigma-Aldrich. Apo-*e*SHMT was prepared using L-cysteine as previously described [8]. The apo-enzyme was stored in 10% glycerol at -20 °C for no more than 3 days before use. The concentration of the apo-*e*SHMT is calculated from an extinction coefficient at 278 nm of 42,790 cm^{-1} M^{-1}. A small, residual fraction (about 5%) of holo-enzyme was always present, as judged by activity assays.

Measurement of PLP molecules bound per monomer of enzyme - Apo-*e*SHMT samples (10 μM in 1 ml) containing PLP at various concentrations (including control samples in which PLP was absent) were prepared in 50 mM HEPES-NaOH buffer at pH 7.2, equilibrated at 30 °C for 30 min and then reduced with $NaBH_4$ (0.2 M). Reduction of PLP-enzyme Schiff base irreversibly links the cofactor to the protein [22]. $NaBH_4$ was prepared as a concentrated solution (2 M) in 50 mM NaOH. After 30 min from $NaBH_4$ addition, samples were concentrated in centrifuge filters (Millipore, Amicon Ultra, cutoff 30 KDa) and diluted with HEPES buffer repeatedly, so as to eliminate small molecular weight molecules, including reduced free cofactor. The final samples were diluted to 1 ml and an absorption spectrum recorded. The A_{335}/A_{280} ratio was calculated, in order to normalise the absorbance of the reduced internal aldimine on the basis of protein concentration, and then divided by the ratio found for a holo-enzyme sample. The result gives the fraction of PLP molecules bound per monomer of enzyme.

Mass spectrometry analysis - Two apo-enzyme samples (10 μM in 1 ml) were incubated with either 40 μM or 600 μM PLP. A third identical control sample did not contain PLP. After 30 min, $NaBH_4$ (0.2 M) was added to the samples. Small size molecules were removed using centrifuge filters as explained in the previous paragraph. Proteolytic digestion of each sample (1.5 μg) was performed adding approximately 0.1 μg of modified porcine trypsin (Millipore) in a solution of 25 mM ammonium bicarbonate and incubated at 37°C overnight. MALDI-

TOF analyses of each tryptic peptide mixture were performed in a Voyager-DETM STR instrument (Applied Biosystem, Framingham, MA, USA).

Activity assays, spectral and stopped-flow studies - The hydroxymethyltransferase activity was measured with L-serine and H_4PteGlu as substrates as previously described [23]. The rate of L-*allo*-threonine cleavage was measured by coupling the reaction with the reduction of the product acetaldehyde by NADH and alcohol dehydrogenase [24].

Absorbance spectra and steady-state kinetic studies were performed on a Hewlett-Packard 8453 diode array spectrophotometer. Fluorescence emission measurements at equilibrium were carried out at 20 °C with a Fluoromax-3 spectrofluorimeter (HORIBA Jobin-Yvon, France), using a 1-cm pathlength quartz cuvette. Pyridoxine 5'-phosphate (PNP) fluorescence emission spectra were recorded from 350 to 500 nm (1-nm sampling interval; 5 nm emission slit) with the excitation wavelength set at 325 nm (1 nm excitation slit); PNP in the cuvette was 2 μM, while apo-*e*SHMT varied between 0.085 and 6 μM. The dissociation constant for the binding equilibrium was calculated from a Scatchard plot [25]. Curve-fitting procedures and statistical analysis were done with Prism (GraphPad Software Inc., San Diego, CA, USA).

Stopped-flow (absorbance and fluorescence) experiments were performed with an Applied Photophysics SX18 apparatus (Leatherhead, UK) equipped with a 1 cm optical path observation chamber. A 360 nm filter was applied when measuring fluorescence emission obtained exciting PNP at 325 nm. Transient spectroscopy experiments were performed with the same apparatus reconfigured with the photodiode-array accessory. All experiments were carried out in HEPES-NaOH buffer, pH 7.2, at 30 °C.

Chemical quenched-flow experiments - The rapid kinetics of internal aldimine formation were analysed by means of quenched-flow experiments carried out on a BioLogic QFM-400 apparatus, using $NaBH_4$ as quencher. Borohydride is known to reduce rapidly and efficiently imines and aldehydes [26]. When the internal aldimine of PLP-dependent enzymes is reduced, the cofactor is irreversibly attached to the protein, giving an absorption spectrum with a band at around 330 nm [27].

The four syringes of the quenched-flow apparatus at 30 °C contained respectively, apo-*e*SHMT (120 μM) in 50 mM HEPES-NaOH buffer at pH 7.2, PLP (20 μM) in the same buffer, water and $NaBH_4$ (2 M) in 50 mM NaOH. In each experiment, equal volumes of apo-

enzyme and PLP (100 μl) were mixed, filling a 200 μl "delay line". Then, water pushed 180 μl of the reaction mixture from the first mixer into the second mixer where it encountered 20 μl of the borohydride solution. The quenched reaction (200 μl) was collected in a vial. The ageing time of reactions was determined by the flow speed through the delay line. Five reactions were carried out for each single ageing time. In the experiments with ageing times longer than one second, the flow was interrupted for the desired time interval once the reaction mixture filled the "delay line", and then started again in order to quench the reaction. After being quenched, reactions were left in the vials for 30 min, in order to dissolve the gas bubbles formed from reaction of borohydride with water. Subsequently, the five samples relative to each ageing time were pooled (1 ml final volume), concentrated in a centrifuge filter and diluted with 50 mM HEPES-NaOH buffer (pH 7.2) repeatedly, so as to eliminate the small molecular weight molecules, including the reduced free cofactor. In the last dilution step, buffer was added to obtain a final volume of 1ml and absorption spectra recorded. The concentration of the reduced internal aldimine was calculated as described above.

Control stopped-flow experiments were carried out in order to compare the rate of $NaBH_4$ reduction of holo-*e*SHMT and free PLP in the aldehyde form. The extrapolated half times of the reactions at 0.2 M $NaBH_4$ (which was the concentration used in the quenched-flow experiments) were calculated to be 0.1 and 3.4 ms, respectively for holo-*e*SHMT and aldehyde PLP.

Data analysis - Binding of PLP to the second site was analysed according to Eqn 1, in which N and K_d stand, respectively, for the number of PLP molecules bound per monomer of enzyme and the apparent dissociation constant of the equilibrium.

Equation 1 $$N = 1 + \frac{[PLP]}{[PLP] + K_d}$$

Fit to Eqn. 2 returned an initial velocity of the reaction in the absence of exogenous PLP (v_0) of 90 ± 3 μM min^{-1} while the velocity at infinite PLP concentration (v_{inf}) was 31 ± 5 μM min^{-1} (at pH 7.2 and 30 °C; holo-enzyme concentration was 0.1 μM).

Equation 2 $$v_i = v_0 - \left((v_0 - v_{\inf}) \times \frac{[PLP]}{[PLP] + K_I} \right)$$

Fit to Eqn. 3 gave an initial velocity in the absence of exogenous PLP of 45 ± 5 μM min^{-1} and a velocity at infinite PLP concentration of 72 ± 6 μM min^{-1} (at pH 7.2 and 30 °C; holo-enzyme concentration was 1.25 μM).

Equation 3 $$v_i = v_0 + \left((v_{\inf} - v_0) \times \frac{[PLP]}{[PLP] + K_A} \right)$$

Equations 1, 2 and 3 are intuitively derived from the following relationship, that may be generally applied to binding equilibria in which the ligand (in our case PLP) is in large excess with respect to the protein [25]:

$$Y = \frac{[PLP]}{[PLP] + K_d};$$

Y is the fraction of enzyme monomers that bind the cofactor at the second binding site, [PLP] is the concentration of free cofactor and K_d is the dissociation constant of the related equilibrium.

Eqn. 4 is the sum of three exponential processes [25].

Equation 4 $$\Delta Abs = A_0 \cdot (1 - \cdot e^{-k_a \cdot t}) + B_0 \cdot (1 - \cdot e^{-k_b \cdot t}) + C_0 \cdot (1 - e^{-k_c \cdot t})$$

In order to evaluate the accuracy of the fit to the sum of either three or two exponential processes, we performed the "F" test and the analysis of the explained variance [28]. A comparison of the fits obtained with either two or three exponentials gave an "F" value of 2.2, that corresponds to a probability of about 5% (one tail; 19 and 14 degrees of freedom, respectively for three and two exponentials; analysis carried out on time courses obtained at the four highest apo-enzyme concentrations). Fits of the same set of data to either one, two or three exponentials gave variances, respectively, of 3.93×10^{-5}, 3.90×10^{-5} and 1.77×10^{-5}, demonstrating a clear-cut decrease of the explained variance with three exponentials. Finally, the distribution of the fit residuals when less than three exponentials were used to fit the data was non-random. These results clearly indicate that data fit better to the sum of three exponentials.

On and off rate constants (k_{on} and k_{off}) for PNP binding kinetics were derived according to Cornish-Bowden [25].

The differential spectra obtained from the rapid scanning experiments were analysed by the singular value decomposition algorithm (SVD) [29] using the software MATLAB (MathWorks Inc., South Natick, MA). The analysis was aimed at determining the number of independent spectral components involved in the reaction. Absorption spectra were placed in a rectangular (m×n) matrix **A**, each column being a spectrum and each row a time course of absorbance at a single wavelength. Matrix **A** was decomposed by SVD into the product of three matrices: $\mathbf{A}=\mathbf{U}\times\mathbf{S}\times\mathbf{V}^T$, where **U** and **V** are orthogonal matrices, and **S** is a diagonal matrix, with its nonzero elements arranged in decreasing order. The columns of matrix **U**

contain the "basis spectra", and those of the **V** matrix contain the time dependence of each "basis spectrum". The diagonal **S** matrix contains the singular values that quantify the relative importance of each corresponding vector in **U**. Each column of matrix **U**×**S** represents a pseudospectrum, i.e. the absorption of one of the spectroscopic components required to approximate the original data and only the first few columns are significant, the last ones having negligibly small values. The signal-to-noise ratio is indeed very high in the earliest columns of **U** and **V**, while the random noise is mainly accumulated in the latest columns.

The global analysis of rapid scanning stopped-flow data and the band shape analysis of absorption spectra were carried out using the software Scientist (Micromath, Saint Louis, MO, USA). Time traces extracted from the hybrid stopped-flow diode array set of data and the kinetics of formation of the internal aldimine were globally fitted by numerical integration to systems of differential equations describing all possible models (made by reversible, unimolecular steps) that would give four independent spectral components when analysed by SVD. Models were made by: i) three consecutive reactions; ii) three parallel reactions; iii) three reactions branching from a single species; iv) two consecutive reactions paralleled by a single reaction. All reasonable combinations of the initial concentrations of components (as well as combinations of components that corresponded to the internal aldimine) were tested. In total, 19 different versions of the four models were tested. Because of the limited capability of the software employed, only nine different time traces (corresponding to the most representative wavelengths) were fitted at once. The capability of the models to fit the data was evaluated on the basis of the distribution of fit residuals. All models but the one made by three consecutive reactions gave clearly non-random residuals. Several different fitting sessions were then carried out according to Scheme I, so as to cover the entire range of wavelengths acquired (95 different wavelengths).We noticed that the parameters produced by the least squares minimization routine were somewhat dependent on the initial estimates. To overcome this problem, the set of time courses was simulated over a wide range of the variable parameters in order to map the variance s^2 in the parameter hyperspace (as suggested by P.R. Bevington [30]). The best parameter sets obtained by this procedure were used as the initial estimates in the minimization routines. Often, but not always, different initial estimates converged to the same minimum. In the end at least two clearly different minima were obtained, and the lower one was chosen as our best description of the experimental data.

RESULTS

Evidence of a second PLP binding site – PLP is a very reactive aldehyde. Before we could analyse the mechanism of PLP addition to *e*SHMT, we had to make sure that we were observing PLP binding only at the active site. The absorption spectrum of PLP changes radically as its aldehyde group forms an aldimine with the ε-amino group of the active site lysine residue (K229 in *e*SHMT), yielding the internal aldimine. A comparison between the spectra of free cofactor and holo-*e*SHMT shows a shift of λ_{max} from 388 nm to 422 nm, with the maximum absorbance change taking place at 435 nm (data not shown). Following the change in absorbance at 435 nm with a stopped-flow spectrophotometer at different apo-enzyme/PLP ratios resulted in complex kinetics (data not shown). Importantly, the shape and amplitude of the absorbance change with a large excess of apo-enzyme (100 μM) over PLP (10 μM) were profoundly different from those obtained with a reversed stoichiometric ratio. In particular, with excess PLP there was a significant increase of the amplitude, suggesting that PLP was adding to at least one additional site.

As a test of this hypothesis, at increasing concentrations of PLP the binding was stoichiometric, until a first site was saturated (Fig. 1, inset). At higher concentrations a second molecule of PLP bound, although with a much lower affinity (Fig. 1). The best fit of data relative to the holo-enzyme to Eqn. 1, which assumes that one molecule of PLP per enzyme monomer is already bound, yielded an apparent dissociation constant (K_d) of 230 ± 60 μM for the binding equilibrium of the second molecule of cofactor at pH 7.2 and 30 °C.

Binding of PLP at the second site had an inhibitory effect on the hydroxymethyltransferase activity (data not shown), with an inhibition constant (K_I), calculated by best fitting the data to Eqn. 2, of 250 ± 100 μM. On the other hand, binding of the second PLP resulted in an increase of the H_4PteGlu-independent L-*allo*-threonine cleavage activity (data not shown). Fitting data to Eqn. 3 returned an activation constant (K_A) of 230 ± 40 μM.

The enzyme residue involved in the covalent binding of PLP to the second site was identified by mass spectrometry analysis of samples of apo-enzyme (10 μM) incubated with either 40 μM or 600 μM PLP. The compared analysis of tryptic peptides showed that the cofactor was bound to Lys 229 in the sample with 40 μM PLP and to both Lys 229 and Lys 346 in the sample with 600 μM PLP.

Single wavelength analysis of holo-eSHMT formation – The finding of a second PLP binding site requires that the studies on the mechanism of addition of PLP be carried out with

an excess of apo-enzyme over cofactor, to minimize complications in determining a kinetic pathway and to maintain pseudo-first-order kinetics. A stopped-flow investigation was carried out, mixing equal volumes of 20 μM PLP with apo-enzyme at several different subunit concentrations (584, 350, 210, 126, 76, 44 and 27.2 μM) and recording absorbance changes at 435 nm (Fig. 2). Kinetic traces resulting from the four higher apo-enzyme concentrations were virtually superimposable and well described by the sum of three exponential processes (Eqn. 4). The sum of two exponential processes did not adequately fit the data, as indicated by the "F" test and the analysis of variance.

Global fitting of the four kinetic traces to Eqn. 4 indicated that the faster exponential process corresponded to a lag phase with a rate constant $k_a = 23.8 \pm 0.9$ s^{-1} and an amplitude $A_0 = -0.0074 \pm .\ 0.0001$ AU (Fig. 2, inset). This was followed by two exponential increases in absorbance at 435 nm, whose rate constants and amplitudes were $k_b = 3.44 \pm 0.03$ s^{-1}, $B_0 = 0.0605 \pm 0.0001$ AU, $k_c = 0.53 \pm 0.02$ s^{-1} and $C_0 = 0.0110 \pm 0.0002$ AU. At apo-enzyme concentrations lower than 126 μM (before mixing), absorbance changes were systematically slower. The observation that k_a does not change above 126 μM subunit concentration rules out that the lag corresponds to the bimolecular binding step. It rather suggests that a rapid equilibrium, corresponding to the binding of PLP to the enzyme, was established in the dead-time of the stopped-flow instrument. Therefore, the lag phase indicates that a reaction intermediate precedes the formation of the 422 nm absorbing internal aldimine.

Rapid scanning analysis of holo-eSHMT formation - The course of the reaction of PLP with apo-*e*SHMT was followed by acquiring spectra with the stopped-flow spectrophotometer in the rapid scanning configuration. Spectra (800) were acquired at 10 ms intervals over a period of 8 s after a 9 ms delay from stop of flow. A control experiment was performed using the same conditions, but with the instrument set up to measure absorbance at a single wavelength (435 nm). Comparison of absorbance changes at 435 nm recorded in the rapid scanning and single wavelength configurations revealed that, when spectra are acquired in the scanning configuration, the absorbance change is smaller and takes place with a different kinetic pattern (data not shown). Traces by the two methods are superimposable up to 1 second, but thereafter diverge. A difference in the single wavelength and rapid scanning methods is the much higher light intensity used in the latter. A repeat of the rapid scanning experiment at a lower light intensity showed that photo bleaching was occurring after 1 s of reaction (400 spectra were acquired at 16 ms intervals over a period of 6.4 s, after a 14 ms delay from stop of flow). However, the low intensity of light in this experiment yielded increased noise in the

data. In order to overcome this problem a hybrid data set was created, gathering the first 25 spectra acquired with intense light (at 10 ms intervals, from 9 ms to 0.26 s after stop of flow) and 385 spectra acquired using low intensity light (at 16 ms intervals, from 0.27 s to 6.4 s after stop of flow) (Fig. 3).

Differential spectra of the hybrid data set (with respect to the last spectrum acquired) were analysed by singular value decomposition (SVD) [29]. The result of the analysis suggested that three independent spectral components were required to describe the experimental data (the S values for the first seven components were 1.36, 0.79, 0.26, 0.18, 0.16, 0.15 and 0.14). Considering that a fourth spectral component has to be added because the analysis was carried out on differential spectra, this interpretation agrees with the single wavelength studies at 435 nm, described by the sum of three exponential processes.

Two additional experiments, that used intense light, were carried out in which either apo-enzyme (120 μM) or PLP (20 μM) were mixed with equal volumes of buffer. No spectral changes were observed in either experiment over a 6 s time period. These experiments gave the spectra of PLP and apo-enzyme after mixing (dashed line in Fig. 3).

PLP in solution is an equilibrium of several different ionic and tautomeric structures with unique absorption properties. At pH 7.2 PLP is mainly present with its ring in the neutral form (about 5% of the cofactor is in the anionic form). Both dipolar ionic (where N_1 is protonated and O_3' is negative) and uncharged tautomers of the neutral ring exist, and each as both aldehyde and hydrate, although the uncharged hydrate is present as a negligible fraction [31]. The spectrum of PLP did not change significantly in the 9 ms after mixing with apo-enzyme (Fig. 3). We conclude that the rapid-binding equilibrium established in the dead-time of the stopped-flow instrument does not alter the distribution of PLP ionic and tautomeric forms. Spectral resolution with log-normal curves permits a quantitative description of equilibria for hydration and tautomerization [32, 33]. The control spectrum of the cofactor after mixing with buffer (which corresponds to the spectrum of PLP at time zero of reaction) was analysed fitting the experimental data points to the sum of the expected component bands, using Metzler's equation. The parameters returned by the fitting were within ± 5% of the values found in the literature. Using the extinction coefficients found in the literature, the analysis showed that the uncharged aldehyde (λ_{max} corresponding to 350 nm) was present as a 28% fraction, while the dipolar ionic aldehyde (388 nm) and the hydrate (323 nm) were present as 52% and 16% fractions, respectively. These values are in agreement with literature values for neutral PLP. A fourth band with an absorbance maximum at around 302 nm had to be included in the calculations in order to obtain a satisfactory fit and may account for the

remaining 4% of the cofactor. This component may be attributed to impurities and to a minor part to the cofactor being in the anionic form, which absorbs at this position. We do not know the exact nature of such impurities, however, the low absorbance maximum may indicate that the carbonyl group is either absent or saturated (and therefore not reactive).

The spectrum of the reaction acquired after 20 ms from stop of flow was also deconvoluted assuming that the absorption bands given by the hydrate form (323 nm) and the material absorbing at 302 nm were unchanged (all related parameters were therefore fixed in the fitting). Only the amplitudes of the bands corresponding to the aldehyde form of the cofactor (350 nm and 388 nm) were left free to vary during the fitting, while the other parameters were fixed to the values found in the previous deconvolution. A fifth absorption band with a maximum at 335 nm had to be included in order to obtain a good fit. This corresponds to a reaction intermediate generated in the very early phase of the reaction. The amplitudes of both bands relative to the aldehyde form of PLP (350 nm and 388 nm) decreased. This analysis suggested that only the aldehyde form of PLP reacts in the first few milliseconds of the reaction, giving the intermediate that absorbs at 335 nm.

Quenched-flow analysis - The formation of the internal aldimine between the PLP aldehyde group and the Lys229 ε-amino group was monitored by chemical quenched-flow experiments in which equal volumes of apo-enzyme (120 μM) and cofactor (20 μM) were rapidly mixed and the reaction quenched at different time intervals with concentrated $NaBH_4$ (0.2 M). This experiment correctly reports the formation of the internal aldimine only if the aldehyde PLP and the internal aldimine are reduced by $NaBH_4$ much more rapidly than the internal aldimine is formed. This point was checked by stopped-flow control experiments, which used either holo-*e*SHMT or free PLP.

The kinetics obtained fitted well to the sum of two exponential processes with rate constants of 38 ± 16 s^{-1} and 0.79 ± 0.15 s^{-1} and amplitudes of 3.1 ± 0.5 μM and 6.4 ± 0.4 μM, respectively (Fig. 4). A constant 0.5 μM internal aldiminine had to be added to account for a small amount of holo-enzyme present as a contaminant in the apo-enzyme samples. Taking into account the large standard deviation of the two rate constants, their values roughly correspond to k_a (23.8 ± 0.9 s^{-1}) and k_c (0.53± 0.02 s^{-1}) of absorbance changes measured at 435 nm in the stopped-flow experiments.

Global analysis – Any kinetic scheme describing the reaction between apo-enzyme and PLP should be consistent with the results of the SVD analysis of the rapid scanning data, which

indicated the presence of four independent spectral components. To begin with, we tested all kinetic models, made by reversible unimolecular steps, that satisfy this requirement, regardless to their consistency with the chemistry of the system under study. Single wavelength traces from the hybrid diode array data and the kinetics of internal aldimine formation were globally fitted to all models. Because of the limits of the software, no more than nine time traces (chosen among the most representative ones) could be fitted at once. Only the model corresponding to three consecutive reactions fitted the data.

A three-step model that is consistent with both our data and the expected mechanism of the reaction is represented by Scheme I, in which PLP_{Ald} and PLP_{Hyd} are the cofactor in the aldehyde and hydrate forms; apoE•PLP_{Ald} and apoE•PLP_{Hyd} are the related non-covalent complexes with the apo-enzyme; E=PLP* is an intermediate internal aldimine and holoE is the holo-enzyme. Fitting data to Scheme I (several fitting sessions were carried out so as to cover the entire range of wavelengths acquired), we assumed that, when the stopped-flow registration of the reaction begins only the species in square brackets are observable and the concentrations of the non-covalent complexes (apoE•PLP_{Hyd} and apoE•PLP_{Hyd}) correspond to those of their related free PLP forms. This assumption is justified by the saturation behaviour observed in the single wavelength experiments (Fig. 2) and the results of band shape analyses. Concentrations of apoE•PLP_{Hyd} and apoE•PLP_{Ald} at time zero were respectively, 1.6 and 8 μM, while those of E=PLP* and holoE were nil. In the global fittings, the concentration of internal aldimine was made equal to the sum of E=PLP* and holoE. The absorbance at any wavelength corresponded to the sum of the concentrations of each of the four kinetic species multiplied by their micromolar extinction coefficient at that wavelength, plus a constant absorbance contributed by the apo-enzyme and the band at 302 nm (found in the band shape analyses and assumed to be mostly inert material; the analysis would have detected any incongruence with this assumption in terms of a poor fit at wavelengths around 302 nm). In the fitting, the extinction coefficients of apoE•PLP_{Hyd} and apoE•PLP_{Ald} were fixed at the values calculated in the band shape analysis of the free cofactor, while those of E=PLP* and holoE were free to vary between zero and infinity. Under the experimental conditions used, either the second or the third reaction (or both) of Scheme I must be virtually irreversible. This hypothesis is confirmed by the observation that all cofactor binds covalently to the apo-enzyme (Fig. 4). The global fit was therefore carried out with three different versions of Scheme I. Only the one in which the third reaction was irreversible fitted the data (Fig. 5),

returning the following rate constants: $k_1 = 1.2\ s^{-1}$, $k_{-1} = 0.3\ s^{-1}$, $k_2 = 18\ s^{-1}$, $k_{-2} = 6.5\ s^{-1}$ and $k_3 = 3.5\ s^{-1}$.

The absorption spectra of the kinetic species, reconstructed from the micromolar extinction coefficients estimated in the fitting, are shown in Fig. 6. The spectrum of the intermediate E=PLP* was deconvoluted into its component bands using Metzler's band shape analysis method (Fig. 7). The main component band has its maximum absorbance at 386 nm. Two additional bands with maxima at 337 and 286 nm, respectively, had to be included in order to obtain a good fit. The other parameters returned by the fitting were within a ± 5% range of the values found in the literature for absorption spectra of PLP-dependent enzymes [34].

Binding of pyridoxine 5'-phosphate to apo-eSHMT – Scheme I assumes that hydrate PLP binds rapidly to apo-*e*SHMT. This hypothesis was tested by following the binding of the structural analogue pyridoxine 5'-phosphate (PNP), which can not proceed further in the reaction sequence because it lacks an aldehyde. PNP does bind to apo-*e*SHMT, as indicated by the increase of this vitamer's fluorescence emission observed upon mixing with the apo-enzyme (data not shown). We calculated a $K_d = 90 \pm 5$ nM for this binding equilibrium. Stopped-flow fluorescence experiments in which 2 μM PNP was mixed with excess apo-enzyme (60 μM), so as to guarantee pseudo-first order conditions, gave biphasic kinetics with apparent rate constants of $178 \pm 4\ s^{-1}$ and $3.21 \pm 0.01\ s^{-1}$ (data not shown). The linear dependence of the faster rate constant on protein concentration indicated that it corresponds to the encounter between PNP and apo-*e*SHMT. The much slower phase that follows is likely to be a conformational change of the enzyme. A $k_{on} = 1.6 \pm 0.4\ s^{-1}\ \mu M^{-1}$ and a $k_{off} = 76 \pm 14\ s^{-1}$ were calculated for the bimolecular step. With 60 μM apo-enzyme (as in the rapid scanning experiments) an observed binding rate constant of about $172\ s^{-1}$ would be measured ($k_{on} \times 60\ \mu M + 76\ s^{-1}$). This means that binding takes place with a half time of about 4 ms, which is not far from the dead time of the stopped-flow instrument (2-3 ms).

DISCUSSION

Second PLP binding site – The apparent dissociation constants calculated in the binding, inhibition and activation experiments are very similar. This suggests that they are relative to the same binding equilibrium. K346, the residue that binds the second PLP molecule, is highly conserved in SHMTs and forms a salt-bridge with the carboxylate group of the glutamyl residue of H_4PteGlu [35]. PLP binding at this site therefore inhibits the folate-dependent serine cleavage reaction. The activation of the folate-independent L-*allo*-threonine cleavage is analogously explained, assuming that PLP binding to K346 mimics H_4PteGlu binding. It was indeed reported by Webb and Matthews [36] that H_4PteGlu stimulates the aldol cleavage reaction. To our knowledge, this second PLP binding site has not been reported previously. Our discovery was incidental and we limited its significance to the design of the kinetic experiments.

Proposed mechanism for PLP addition to apo-eSHMT – Before the reaction begins, the free cofactor is present as an equilibrium mixture of hydrate and aldehyde forms (PLP_{Hyd} and PLP_{Ald} in Scheme I). Upon mixing PLP and apo-enzyme, a rapid non-covalent binding equilibrium is established in the dead-time of the stopped-flow instrument. Scheme I assumes that both hydrate and aldehyde PLP binds rapidly to the apo-enzyme. This assumption is well substantiated. The solution rate constant for interconversion of PLP_{Hyd} and PLP_{Ald} at pH 7.0 and 25 °C has been reported to be around 10 s^{-1} [37]. We found it to be 16 s^{-1} in the buffer used for our experiments at pH 7.2 and 30 °C (data not shown). This rate constant is not observed in either the single wavelength or rapid scanning kinetic results in our binding studies. This suggests that hydrate PLP binds to the enzyme. Moreover, we showed that PNP, a good structural analogue of hydrate PLP, binds rapidly to the apo-enzyme.

The rate constants determined for Scheme I from the rapid scanning data compare favourably with those obtained for the single wavelength studies. The values of k_1, k_{-1} k_2, k_{-2} and k_3 make it clear that the complex of the enzyme with PLP_{Ald} (apoE•PLP_{Ald}) reacts much faster than the corresponding complex with the hydrate (apoE•PLP_{Hyd}). Thus, upon combination of the cofactor with the apo-enzyme, the apoE•PLP_{Ald} complex evolves to the equilibrium species (E=PLP*) before apoE•PLP_{Hyd} decays to any significant extent. Therefore, the apparent rate constants k_a (23.8 s^{-1}) and k_b (3.44 s^{-1}) from the single wavelength studies roughly correspond, respectively, to the sum of the intrinsic rate constants k_2+k_{-2} (18 s^{-1} + 6.5 s^{-1}) and to k_3 (3.5 s^{-1}). The slowest exponential process, dominated by k_c (0.53 s^{-1}),

represents the decay of apoE•PLP_{Hyd}, which corresponds to the conversion of the enzyme-bound hydrate PLP (apoE•PLP_{Hyd}) to the enzyme-bound aldehyde form (apoE•PLP_{Ald}). Alternatively, it may correspond to the dissociation of hydrate PLP from the enzyme, its dehydration and binding to the apo-enzyme as aldehyde.

The absorbance change at 435 nm reports the formation of the holo-enzyme (holoE). There is a pronounced lag in the formation of holoE in the stopped-flow studies (Fig. 2, inset). Within experimental error, the rate of the burst in the quench-flow studies (Fig. 4) is the same as the lag in the rapid reaction studies. This suggests that holoE is formed from an intermediate aldimine species not absorbing at 435 nm (shown as E=PLP* in Scheme I).

The spectrum of E=PLP* has a major absorption band with a maximum at 386 nm (Fig. 7). Protonated aldimines are normally observed to have maximum absorption between 410 nm and 430 nm. However, aldimines absorbing between 385 and 400 nm have been reported in the literature [38-40]. In particular, evidence was presented that in the aspartate aminotransferase Y225F mutant at high pH, the chromophore absorbing maximally at 386 nm was the unprotonated internal aldimine [41, 42]. In this case, the maximum absorbance of the unprotonated aldimine, usually positioned at around 360 nm, was shifted to higher wavelengths due to the alteration of the active site environment caused by the mutation. The unusual absorption maximum at 386 nm of the E=PLP* aldimine suggests that the incompletely formed active site of apo-*e*SHMT may also bind PLP as an unprotonated aldimine. A smaller absorption peak is also observed at 337 nm for E=PLP* (Fig. 7). This may be attributed to an enolimine tautomer, or more likely to a required carbinolamine intermediate that is in rapid equilibrium with the aldimine [43].

The final step in Scheme I (E=PLP* going to holo-E) is most likely a conformational change. This step is predicted to be largely irreversible, trapping the PLP in its deep cleft as revealed from its crystal structure. Interestingly, the slower fluorescence change associated to PNP binding to apo-*e*SHMT takes place with a similar rate constant, suggesting that the final conformational change may be independent from the internal aldimine formation.

Our future studies will be aimed at answering several key questions raised by the proposed mechanism shown in Scheme I. The first one concerns the structural features the cofactor requires in order to form the first non-covalent complex with the apo-enzyme and then trigger the conformational change that yields the holo-enzyme. Do aldimines of PLP with amino acids bind? Does *e*SHMT bind the aldimines of its substrates glycine and serine selectively with respect to aldimines of non-substrate amino acids? What is the K_d of the first binding equilibrium? Logic would predict that the first complex formed by the apo-enzyme

with PLP would result in a relatively low K_d, so that PLP would not be sequestered by the cell cytoplasm, where this very reactive aldehyde is subject to reactions with a host of nucleophiles. In the cell there may be little PLP_{Ald}. Most of it is likely present as aldimines with amino acids or complexes with thiol compounds [10]. Studies on PNP binding gave a K_d of about 47 μM for the first binding equilibrium of (k_{off}/k_{on}).

Other interesting questions relate to the role of K229 in the final conformational change (E=PLP* going to holo-E) and the structure of apo-*e*SHMT. The first one may be answered by studies on site-specific mutants. Folding studies suggest that an N-terminal segment and an interdomain loop that form part of the active site are both exposed to solvent in a folding intermediate that precedes the formation of apo-*e*SHMT. May be these structural elements of the protein are still exposed in apo-*e*SHMT and E=PLP*.

ACKNOWLEDGEMENTS

We thank Professor Verne Schirch for his precious help in planning, discussing the experiments and help in writing the manuscript. We also thank Amleto Ballini for his technical support and Renata Quattrini, an undergraduate student participant. We are grateful to Eprova AG, Schaffhausen, Switzerland, for providing pure (6*S*) H_4PteGlu. This work was supported by grants of the Italian Ministero dell'Università e della Ricerca.

REFERENCES

1 Higgins, C. L., Muralidhara, B. K. and Wittung-Stafshede, P. (2005) How do cofactors modulate protein folding? Protein. Pept. Lett. **12**, 165-170

2 Wittung-Stafshede, P. (2002) Role of cofactors in protein folding. Acc. Chem. Res. **35**, 201-208

3 Wittung-Stafshede, P. (2004) Role of cofactors in folding of the blue-copper protein azurin. Inorg. Chem. **43**, 7926-7933

4 Bettati, S., Benci, S., Campanini, B., Raboni, S., Chirico, G., Beretta, S., Schnackerz, K. D., Hazlett, T. L., Gratton, E. and Mozzarelli, A. (2000) Role of pyridoxal 5'-phosphate in the structural stabilization of O-acetylserine sulfhydrylase. J. Biol. Chem. **275**, 40244-40251

5 Groha, C., Bartholmes, P. and Jaenicke, R. (1978) Refolding and reactivation of Escherichia coli tryptophan synthase beta2 subunit after inactivation and dissociation in guanidine hydrochloride at acidic pH. Eur. J. Biochem. **92**, 437-441

6 Herold, M. and Leistler, B. (1992) Coenzyme binding of a folding intermediate of aspartate aminotransferase detected by HPLC fluorescence measurements. FEBS Lett. **308**, 26-29

7 Bertoldi, M., Cellini, B., Laurents, D. V. and Borri Voltattorni, C. (2005) Folding pathway of the pyridoxal 5'-phosphate C-S lyase MalY from Escherichia coli. Biochem. J. **389**, 885-898

8 Cai, K., Schirch, D. and Schirch, V. (1995) The affinity of pyridoxal 5'-phosphate for folding intermediates of Escherichia coli serine hydroxymethyltransferase. J. Biol. Chem. **270**, 19294-19299

9 Grishin, N. V., Phillips, M. A. and Goldsmith, E. J. (1995) Modeling of the spatial structure of eukaryotic ornithine decarboxylases. Protein Sci. **4**, 1291-1304

10 Fu, T. F., di Salvo, M. and Schirch, V. (2001) Distribution of B6 vitamers in Escherichia coli as determined by enzymatic assay. Anal. Biochem. **298**, 314-321

11 Cai, K. and Schirch, V. (1996) Structural studies on folding intermediates of serine hydroxymethyltransferase using fluorescence resonance energy transfer. J. Biol. Chem. **271**, 27311-27320

12 Cai, K. and Schirch, V. (1996) Structural studies on folding intermediates of serine hydroxymethyltransferase using single tryptophan mutants. J. Biol. Chem. **271**, 2987-2994

13 Fu, T. F., Boja, E. S., Safo, M. K. and Schirch, V. (2003) Role of proline residues in the folding of serine hydroxymethyltransferase. J. Biol. Chem. **278**, 31088-31094

14 Scarsdale, J. N., Radaev, S., Kazanina, G., Schirch, V. and Wright, H. T. (2000) Crystal structure at 2.4 A resolution of E. coli serine hydroxymethyltransferase in complex with glycine substrate and 5-formyl tetrahydrofolate. J. Mol. Biol. **296**, 155-168

15 Churchich, J. E. and Farrelly, J. G. (1968) Reconstitution of aspartate aminotransferase from pig heart. Biochem. Biophys. Res. Commun. **31**, 316-321

16 Verge, D. and Arrio-Dupont, M. (1981) Interactions between apoaspartate aminotransferase and pyridoxal 5'-phosphate. A stopped-flow study. Biochemistry. **20**, 1210-1216

17 Toney, M. D. and Kirsch, J. F. (1991) Kinetics and equilibria for the reactions of coenzymes with wild type and the Y70F mutant of Escherichia coli aspartate aminotransferase. Biochemistry. **30**, 7461-7466

18 O'Leary, M. H. and Malik, J. M. (1972) Kinetics and mechanism of the binding of pyridoxal 5'-phosphate to apoglutamate decarboxylase. Evidence for a rate-determining conformation change. J. Biol. Chem. **247**, 7097-7105

19 Erez, T., Phillips, R. S. and Parola, A. H. (1998) Pyridoxal phosphate binding to wild type, W330F, and C298S mutants of Escherichia coli apotryptophanase: unraveling the cold inactivation. FEBS Lett. **433**, 279-282

20 Iurescia, S., Condo, I., Angelaccio, S., Delle Fratte, S. and Bossa, F. (1996) Site-directed mutagenesis techniques in the study of Escherichia coli serine hydroxymethyltransferase. Protein Expr. Purif. **7**, 323-328

21 Schirch, V. (1997) Purification of folate-dependent enzymes from rabbit liver. Methods Enzymol. **281**, 146-161

22 Fischer, E. H., Kent, A.B, Snyder, E.R., and Krebs, E.G. (1958) The reaction of sodium borohydrate with muscle phosphorylase. J. Am. Chem. Soc. **80**, 2906-2907

23 Schirch, V., Hopkins, S., Villar, E. and Angelaccio, S. (1985) Serine hydroxymethyltransferase from Escherichia coli: purification and properties. J. Bacteriol. **163**, 1-7

24 Schirch, L. and Peterson, D. (1980) Purification and properties of mitochondrial serine hydroxymethyltransferase. J. Biol. Chem. **255**, 7801-7806

25 Cornish-Bowden, A. (1995) Fundamentals of enzyme kinetics, pp. 1-6, 216, 289, Portland, London

26 Hajâos, A. (1979) Complex hydrides and related reducing agents in organic synthesis. Elsevier Scientific Pub. Co. ; New York

27 Hughes, R. C., Jenkins, W. T. and Fischer, E. H. (1962) The site of binding of pyridoxal-5'-phosphate to heart glutamic-aspartic transaminase. Proc. Natl. Acad. Sci. U S A. **48**, 1615-1618

28 Motulsky, H. (1995) Intuitive biostatistics. Oxford University Press, New York ; Oxford

29 Henry, E. R. a. J. H. (1992) Singular value decomposition: application to analysis of experimental data. Methods Enzymol. **210**, 129-193.

30 Bevington, P. R. (1969) Data reduction and error analysis for the physical sciences, p. 206, McGraw-Hill, New York ; London

31 Harris, C. M., Johnson, R. J. and Metzler, D. E. (1976) Band-shape analysis and resolution of electronic spectra of pyridoxal phosphate and other 3-hydroxypyridine-4-aldehydes. Biochim. Biophys. Acta **421**, 181-194

32 Metzler, D. E., Harris, C. M., Johnson, R. J., Saino, D. B. and Thomson, J. A. (1973) Spectra of 3-hydroxypyridines. Band-shape analysis and evaluation of tautomeric equilibria. Biochemistry. **12**, 5377-5392

33 Johnson, R. J. a. M., D.E. (1970) Analyzing spectra of vitamin B6 derivatives. Methods Enzymol. **18A**, 433-471

34 Metzler, C. M. and Metzler, D. E. (1987) Quantitative description of absorption spectra of a pyridoxal phosphate-dependent enzyme using lognormal distribution curves. Anal. Biochem. **166**, 313-327

35 Fu, T. F., Scarsdale, J. N., Kazanina, G., Schirch, V. and Wright, H. T. (2003) Location of the pteroylpolyglutamate-binding site on rabbit cytosolic serine hydroxymethyltransferase. J. Biol. Chem. **278**, 2645-2653

36 Webb, H. K. and Matthews, R. G. (1995) 4-Chlorothreonine is substrate, mechanistic probe, and mechanism-based inactivator of serine hydroxymethyltransferase. J. Biol. Chem. **270**, 17204-17209

37 Ahrens, M. L., Maass, G., Schuster, P. and Winkler, H. (1970) Kinetic study of the hydration mechanism of vitamin B6 and related compounds. J. Am. Chem. Soc. **92**, 6134-6139

38 Minelli, A., Charteris, A. T., Voltattorni, C. B. and John, R. A. (1979) Reactions of DOPA (3,4-dihydroxyphenylalanine) decarboxylase with DOPA. Biochem. J. **183**, 361-368

39 Hayashi, H., Mizuguchi, H. and Kagamiyama, H. (1993) Rat liver aromatic L-amino acid decarboxylase: spectroscopic and kinetic analysis of the coenzyme and reaction intermediates. Biochemistry. **32**, 812-818

40 Hayashi, H., Tsukiyama, F., Ishii, S., Mizuguchi, H. and Kagamiyama, H. (1999) Acid-base chemistry of the reaction of aromatic L-amino acid decarboxylase and dopa analyzed by transient and steady-state kinetics: preferential binding of the substrate with its amino group unprotonated. Biochemistry. **38**, 15615-15622

41 Goldberg, J. M., Zheng, J., Deng, H., Chen, Y. Q., Callender, R. and Kirsch, J. F. (1993) Structure of the complex between pyridoxal 5'-phosphate and the tyrosine 225 to phenylalanine mutant of Escherichia coli aspartate aminotransferase determined by isotope-edited classical Raman difference spectroscopy. Biochemistry. **32**, 8092-8097

42 Goldberg, J. M., Swanson, R. V., Goodman, H. S. and Kirsch, J. F. (1991) The tyrosine-225 to phenylalanine mutation of Escherichia coli aspartate aminotransferase results in an alkaline transition in the spectrophotometric and kinetic pKa values and reduced values of both kcat and Km. Biochemistry. **30**, 305-312

43 Kallen, R. G., Korpela, T., Martell, A.E., Matsushima, Y., Metzler, C.M., Metzler, D.E., Morozov, Y.V., Ralston, I.M., Savin, F.A., Torchinsky, Y.M., and Ueno, I. (1985) Chemical and spectroscopic properties of pyridoxal and pyridoxamine phosphates, in Transaminases, Wiley-Interscience, NY

FIGURE LEGENDS

FIGURE 1. **Equilibrium binding of PLP to *e*SHMT.** The number of PLP molecules bound per monomer of enzyme (10 μM) was measured as a function of cofactor concentration in 50 mM HEPES-NaOH buffer, pH 7.2, at 30 ºC. The continuous line through the experimental points (○, apo-enzyme; ●, holo-enzyme) derived from the best fit of data to Eqn 1. The inset shows the different behaviour of apo- and holo-enzyme at low PLP concentration.

FIGURE 2. **Absorbance changes at 435 nm observed upon stopped-flow mixing apo-enzyme and PLP.** Absorbance changes at 435 nm upon stopped-flow mixing equal volumes of 584 μM, 350 μM, 210 μM, 126 μM (——), 76 μM (-----), 44 μM (·····), 27.2 μM (-·-·-·-·) apo-enzyme and 20 μM PLP. Conditions were as in Fig.1. The inset shows the lag phase.

FIGURE 3. **Spectral changes observed upon stopped-flow mixing 120 μM apo-enzyme and 20 μM PLP.** Only spectra taken at 20 ms intervals (after 9 ms from stop of flow) with intense light and at 64 ms intervals with low intensity light are shown for clarity. The sum of the spectra of PLP and apo-enzyme obtained after mixing with buffer is shown as a thick, dashed line. Conditions were as in Fig.1.

FIGURE 4. **Kinetics of Schiff base formation between 10 μM PLP and 60 μM apo-enzyme, using chemical quenched-flow.** The experimental points represent covalently bound PLP and the theoretical line is from fitting to the sum of two exponential processes. Conditions were as in Fig.1. The inset shows the burst in the early phase of the reaction.

FIGURE 5. **Representative results of the global fit of absorbance changes and internal aldimine formation.** *Upper panel* - Internal aldimine formation (symbols) and nine kinetic traces (only three of which are shown for clarity in the inset) were fitted by least squares to differential equations corresponding to Scheme I. *Middle panel* - Expanded view showing the early phase of the reaction. *Lower panel* - residuals of the fit relative to all nine kinetic traces and the internal aldimine formation.

FIGURE 6. **Absorption spectra of kinetic species in Scheme I, as reconstructed from the estimated extinction coefficients yielded by the global fit.** apo-E●PLP_{Hyd} (——), apo-E●PLP_{Ald} (-----), E=PLP* (·····) and holo-E (·-·-·-).

FIGURE 7. **Band shape analysis of the absorption spectrum of the intermediate holoenzyme.** The reconstructed spectrum of E=PLP* (×) was deconvoluted into its component bands (continuous lines) with absorption maxima at 386 nm, 337 nm and 286 nm. The inset shows the residuals of the fit.

Biochemical Journal Immediate Publication. Published on 6 Mar 2007 as manuscript BJ20061681

Scheme I

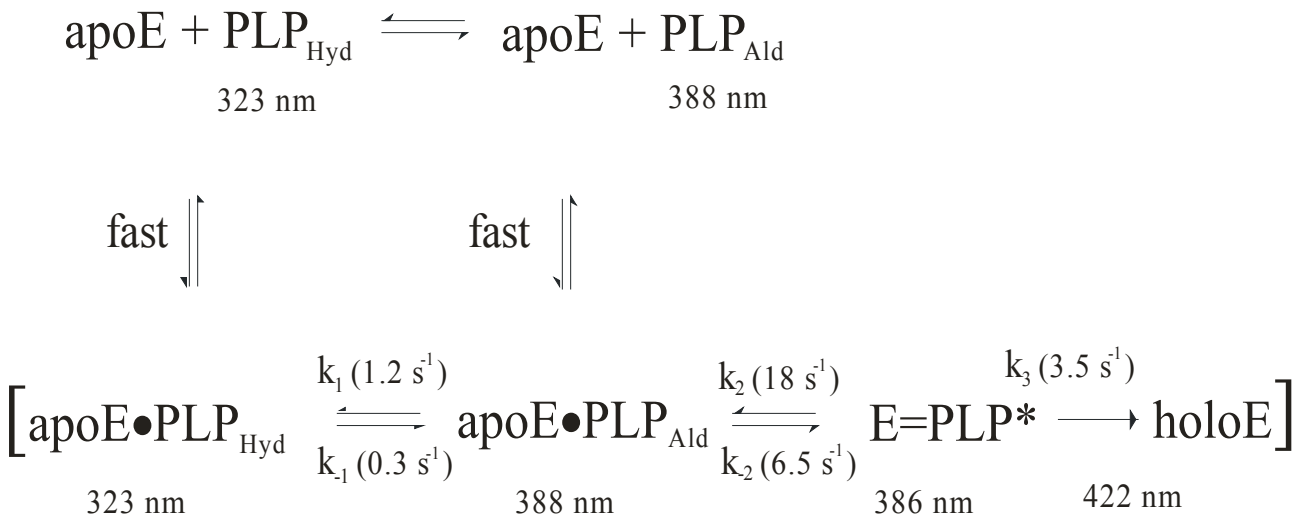

Figure 1

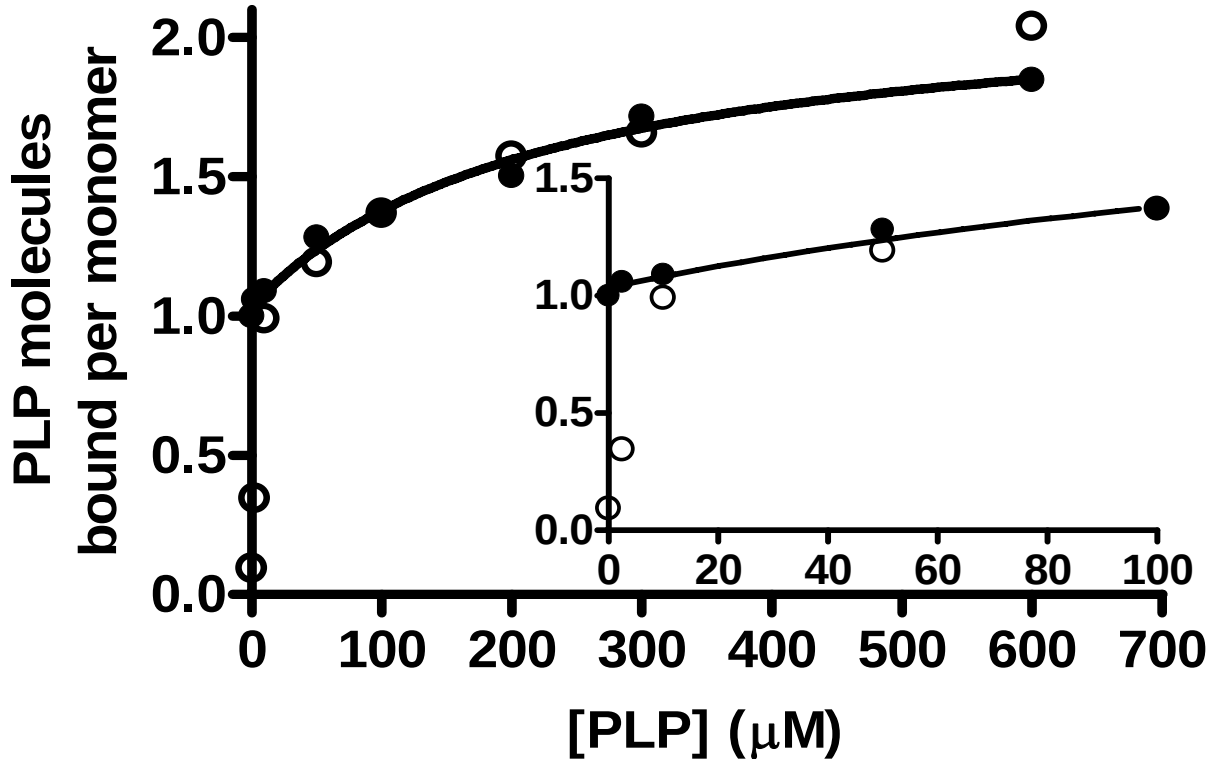

Biochemical Journal Immediate Publication. Published on 6 Mar 2007 as manuscript BJ20061681

Figure 2

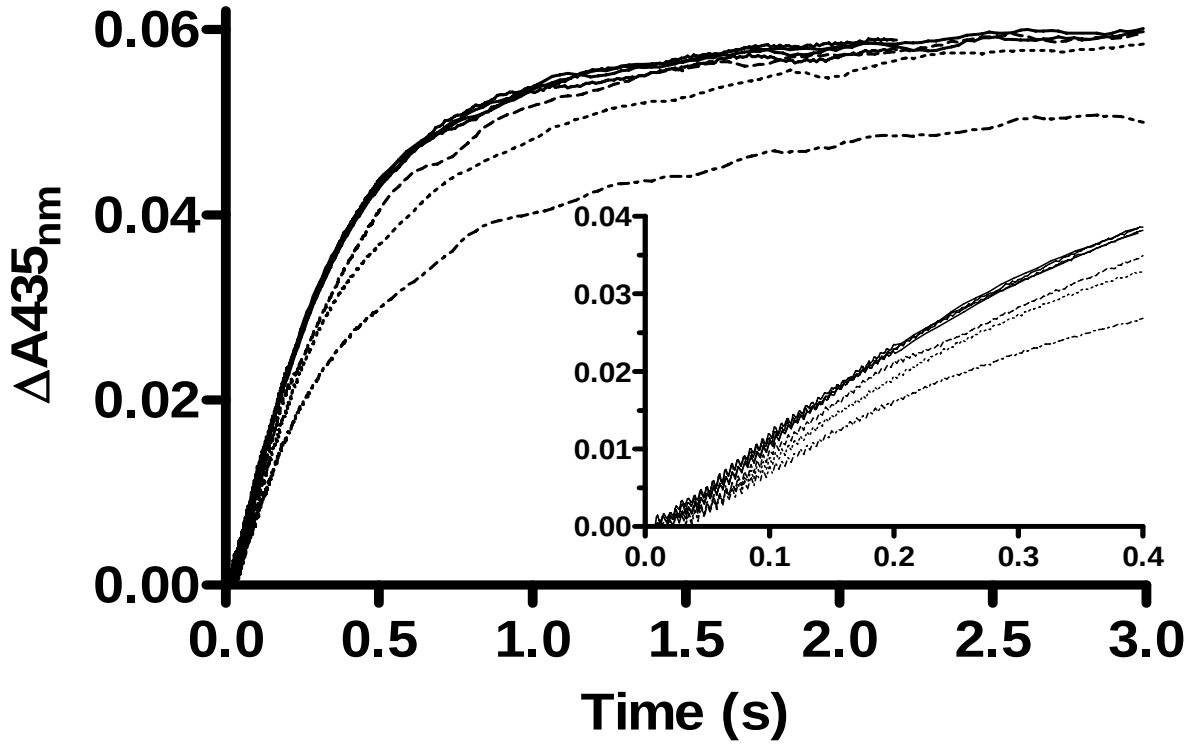

Biochemical Journal Immediate Publication. Published on 6 Mar 2007 as manuscript BJ20061681

Figure 3

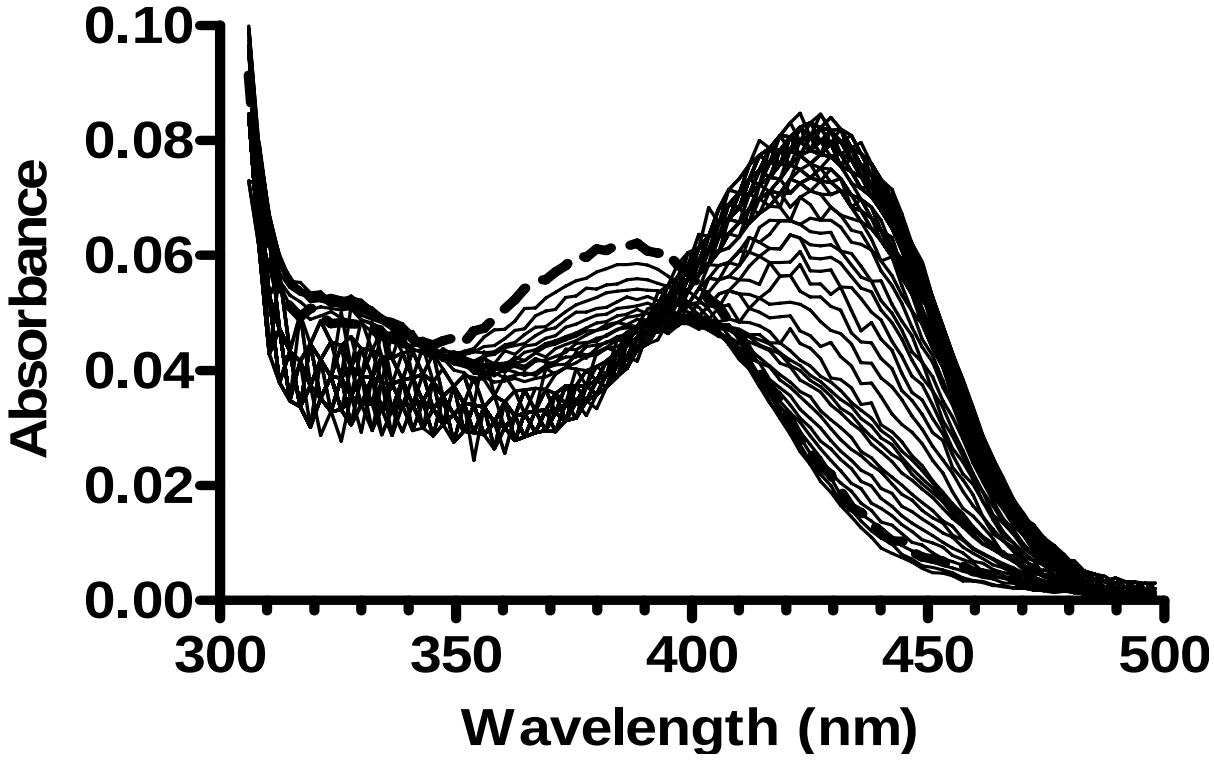

Biochemical Journal Immediate Publication. Published on 6 Mar 2007 as manuscript BJ20061681

Figure 4

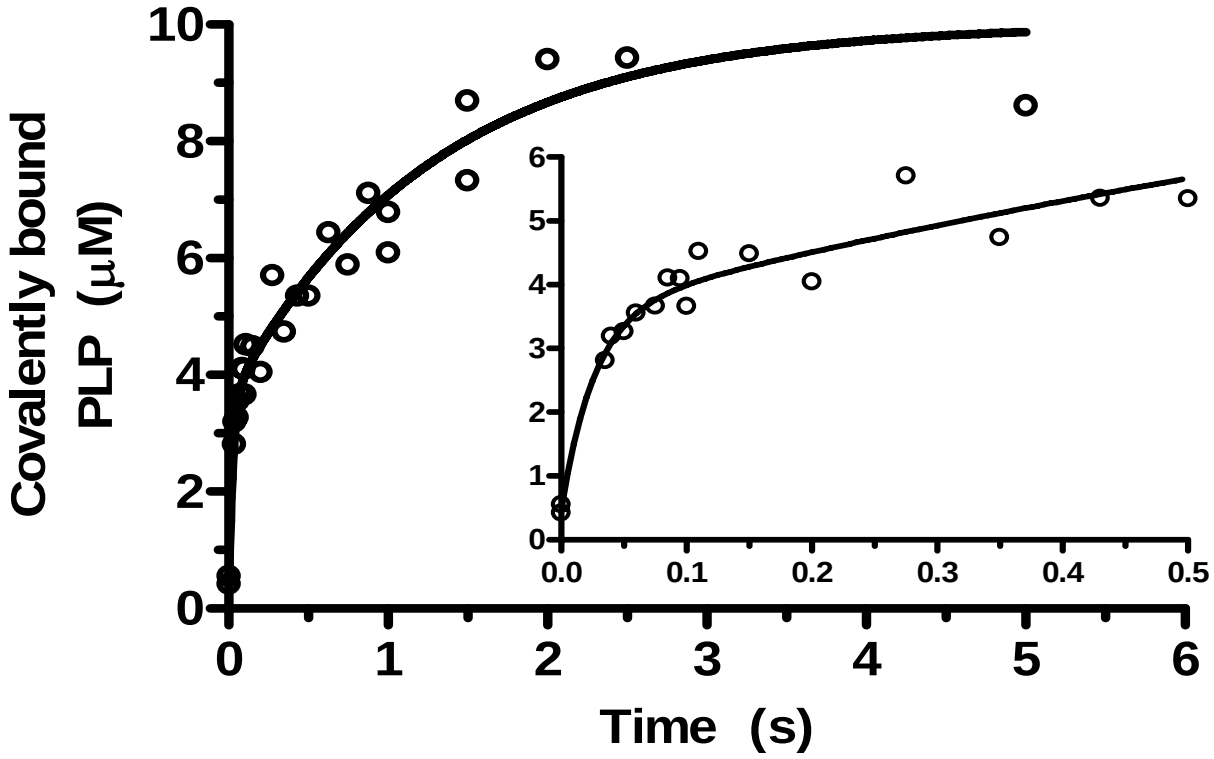

Biochemical Journal Immediate Publication. Published on 6 Mar 2007 as manuscript BJ20061681

Figure 5

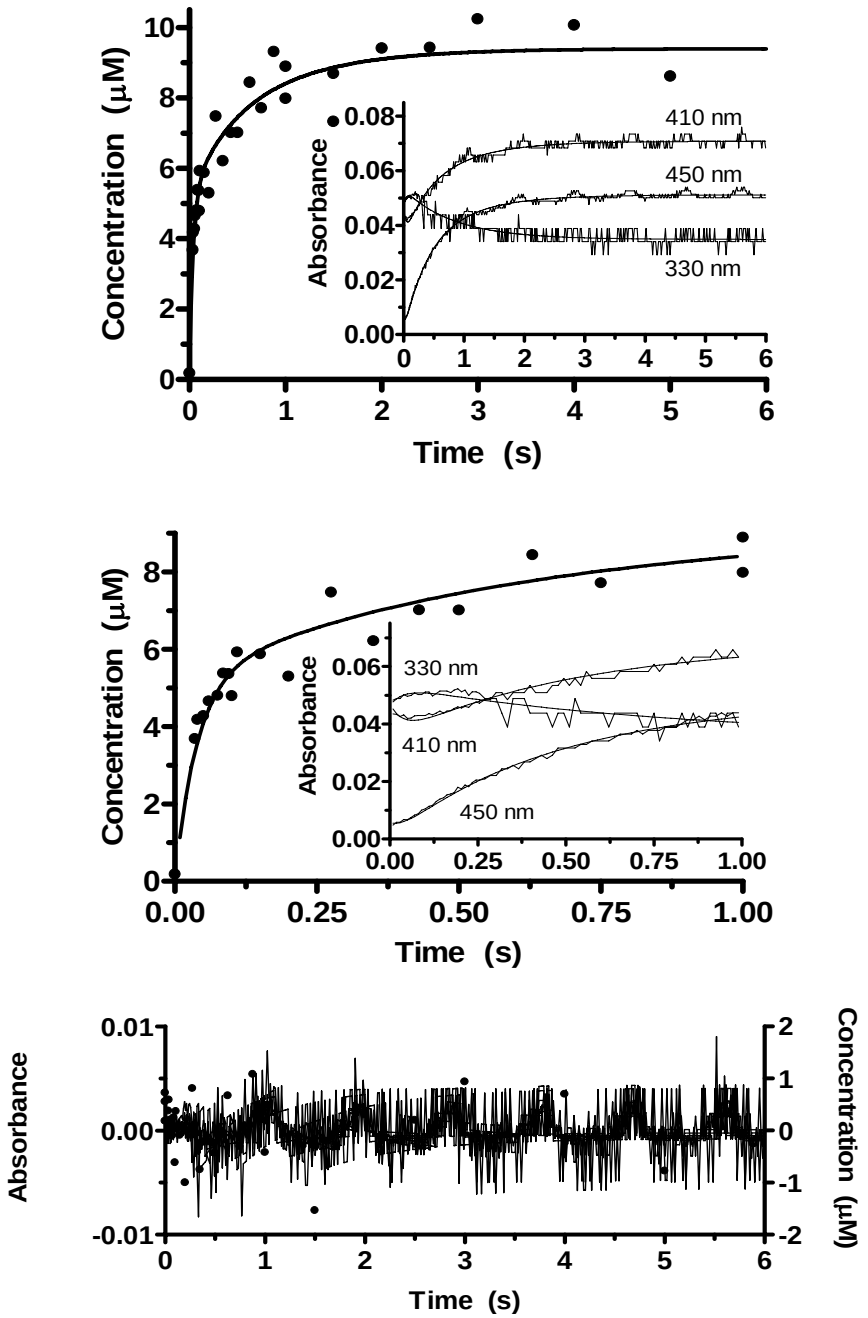

Figure 6

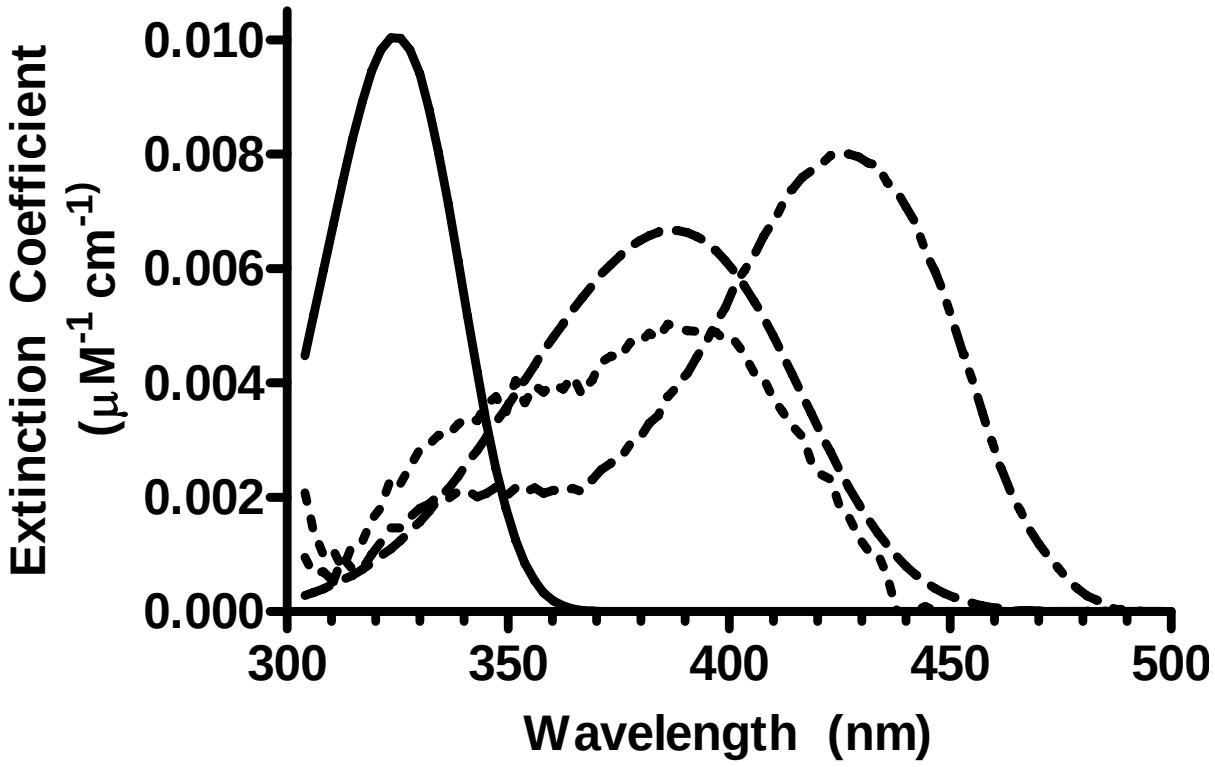

Figure 7